The International Journal of Engineering and Science (IJES)
|| Volume || 8 || Issue || 9 Series I || Pages || PP 11-20 || 2019 ||
ISSN (e): 2319 – 1813 ISSN (p): 23-19 – 1805

Modeling and Evaluation of Leakage Current Behavior of Metal oxide Surge Arresters under Various Applied Voltages and Polluted Conditions

J.O. Aibangbee[1] and S.O. Ikheloa [2]
[1]*Department of Electrical/Electronic & Computer Engineering, Bells University of Technology, Ota, Ogun State, Nigeria*
[2]*Department of Electrical Technology, National Institute of Construction Technology, Uromi, Nigeria*
Corresponding Author: J.O. Aibangbee

----------ABSTRACT: ----------
In this study, the effect of different applied voltages, wetness and polluted conditions on the surge arrester leakage current was evaluated using measurements and simulation models. In metal oxide surge arresters, leakage current usually flows across the arrester under normal operating condition. Leakage current is one of the factors which contribute towards degradation of surge arresters. The behavior of leakage current in a metal oxide surge arrester during normal operation, under different voltages, wetness and pollution conditions were analyzed. An 11 kV surge arrester model in three-dimensional space was subjected to finite element analysis (FEA) to determine the leakage current under different conditions. The results from the FEA developed model of the surge arrester revealed that the material conductivity affects the leakage current significantly under different applied voltages, wetness conditions and pollution conditions. The results from the FEA model were compared with the measurement results to validate the model that has been developed. From comparison between the measurement and simulation results, physical parameters of a surge arrester that influence the leakage current under different conditions of the surge arrester were identified from the model. Through this study, a better understanding of leakage current behavior can be attained, which will help in condition monitoring analysis on surge arrester in electrical utilities.
KEY WORDS: *Leakage current; Finite Element Analysis; Metal oxide; Surge arrester; Applied Voltages; Pollution.*

Date of Submission: 30-08-2019 Date of acceptance: 16-09-2019

I. INTRODUCTION

Transient overvoltage studies are very important for electrical power engineering either for economic design of electrical apparatus or operational reliability of the system. This phenomenon is caused mainly either by lightning strikes or switching operation. Lightning overvoltage's are caused either by direct strokes to the phase conductor of a transmission line, or as a result of strokes to earth very closed to the line which produces induced lightning surges. The overvoltage by which substation insulation is stressed is a function of the line construction and the system configuration. One of the ways to protect the transmission line from lightning overvoltage is by installing surge arresters [1, 2]. A surge arrester limits the peak overvoltage to a level which will protect the instrument from damage [3, 4, 5]. The usual types of surge arresters are silicon carbide arresters with spark gaps, silicon carbide arresters with current limiting gaps and gapless metal oxide also known as zinc oxide (ZnO) arresters. Unfortunately, arresters with spark gaps are not very suitable to limit the switching overvoltage. The degradation of zinc oxide surge arresters is caused by many factors, but one of the main ones is moisture ingress due to weakening of the housing sealing which can lead to internal discharges [6], increasing of electric field around the surge arrester and overheating of the surge arrester. A leakage current always flows across arresters under normal condition. Leakage currents can be categorized as resistive and capacitive component currents. Capacitive component currents are due to the grading capacitor, stray capacitance or permittivity of the ZnO elements. Resistive components are due to pollution of ZnO elements. The resistive current will increase with time, ambient temperature and applied voltage [7]. Thus, it is very important to monitor the leakage current behavior in order to reduce the degradation of ZnO surge arresters. Since leakage currents are influenced by various surge arrester parameters, many studies have been performed on the leakage current behavior under many circumstances. In general, these can be divided into two methods: offline and on-line.

Among these methods, a helpful indication of the surge arrester condition is based on the calculation of its resistive current [8]. Measurements of capacitive and resistive leakage currents have become imperative.

Therefore, several methods for extracting resistive leakage current from the total leakage current have been proposed by many academia's. There are the current orthogonally method (COM) [9], current compensation method (CCCM) [10], point on- wave method (POWM) [11], resistive current wave shape-based method (RCWM) [12], harmonic analysis method (HAM), time delay addition method (TDAM) and improved time delay addition method (ITDAM) [13].

II. DESCRIPTION

The metal oxide gapless surge arresters is a semiconductor device made of a ceramic resistor material constituting ZnO and oxides of other metals, such as bismuth, cobalt, antimony and manganese. These ingredients in different proportions are mixed in powdered form, ZnO being the main ingredient. The material for non-linear resistance used in the manufacture of an efficient surge protection device offer the least impedance during a discharge. This is to provide a free flow to the excessive discharge current to the ground, and to draw a negligible current under normal system conditions, to make it a low-loss device. The basic molecular structure is a matrix of highly conductive ZnO grains surrounded by resistive inter-granular layers of zinc oxide or metal oxide elements as shown in Figure 1(a).

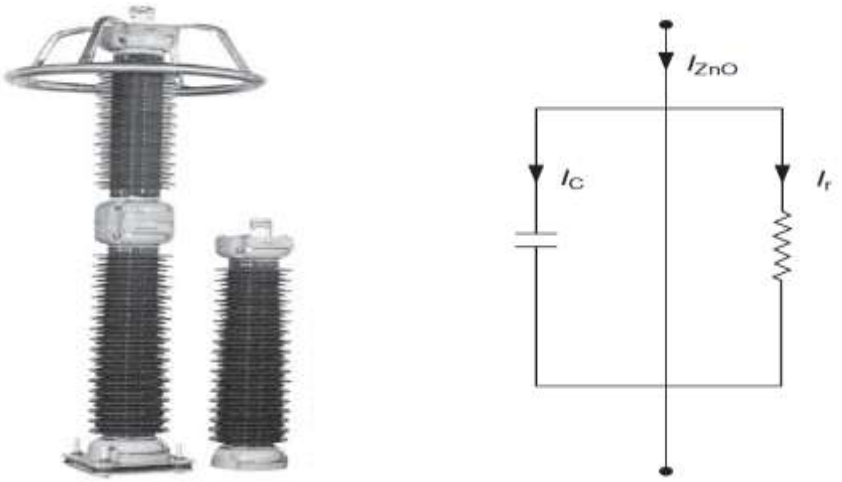

Figure 1 (a) Metal Oxide Surge Arrester (b) Electrical Representation of ZnO element.
Source: …ABB, India 1991.

A ZnO element basically represents a capacitive leakage circuit. In its leakage current range, it may be electrically represented as shown in Figure 1(b), where IZnO is the leakage current, capacitive in nature, and Ic and Ir are capacitive and loss components, respectively. Metal oxide surge arrester is highly non-linear resistor, with an almost infinite slope in the normal-voltage region, and an almost horizontal slope in the overvoltage protection region. Additionally at fast rising voltage, the protective characteristic of the Metal-Oxide surge arrester is superior, because the turn-on characteristic is not determined by series gap [14,15]. As protective device the primary function of Metal-Oxide surge arrester is to protect transmission line and distribution equipment from overvoltage and to absorb electrical energy resulting from the lightning or switching surges or temporary overvoltage [16]. Thus the surge arresters should satisfy these three conditions viz: 1) withstand continuity of the power frequency and voltage at which it is attended to operate; 2) Limit overvoltages on electric power systems by discharging transient energy in the form of current, and 3) operate in the same environment as the protected equipment. Metal-Oxide surge arresters generally have the characteristics that its residual voltage rises for current impulse having steeper front than standard impulse current (8/20μs). Rising rate of residual voltage depends on the time to crest, peak value of the current and kinds of models. Metal-Oxide surge arresters offer a lot of improvements and advantages over Silicon-Carbide surge arresters as summarized to includes (a) Extreme non-linearity (flatness) of V-I characteristics, (b) Elimination of the requirement for a series gap and associated gap spark over voltage (c) The absence of the gap means that under step overvoltage conditions there is no need to consider the volt-time gap spark over characteristics, (d) Volume reduced by as much as 60 percent since gaps and grading components are eliminated, (e) Gapless arresters are much less prone to deterioration in performance due to high surface contamination because there is no gap spark over consideration [17,18, 19].

III. MATERIALS AND METHODS

The development of the models in finite element analysis (FEA), leakage current measurement setup, and preparation of the test samples, leakage current calculation using FEA model and extraction method of resistive leakage current are analyzed. The dimensions and parameters of the ZnO surge arrester used in this study are shown in Table 1.

Table 1: Dimensions and parameters of the surge arrester

	Characteristics	**Data**
1	Creepage distance	344mm
2	Dimensions (L × B × H)	39 × 29 × 26 cm
3	Height	227 mm
4	Housing material	Silicon rubber
5	MCOV	10 kVrms
6	Net weight	1.86 kg
7	Nominal discharge current, In 8/20 µs	10 kA peak
8	Number of sheds	4
9	Rated voltage	12.5 kVrms

3.1. Leakage Current Measurement Setup

The measurement setup consists of a sinusoidal variable voltage source, a high voltage step-up transformer of 0.415/11 kV, a 2.4 MΩ protective resistor (Rs) to prevent short circuit, a 1 nF measuring capacitor (C1) to observe the applied voltage, a measuring circuit, a 20 kΩ shunt resistor (Rsh) to measure the leakage currents by measuring the voltage drop from the current built across the resistance and a two channel digital storage oscilloscope to capture the applied voltage and current through a silicone rubber-housed surge arrester. Figure 2 shows the leakage current measurement setup on the ZnO surge arrester used in the laboratory.

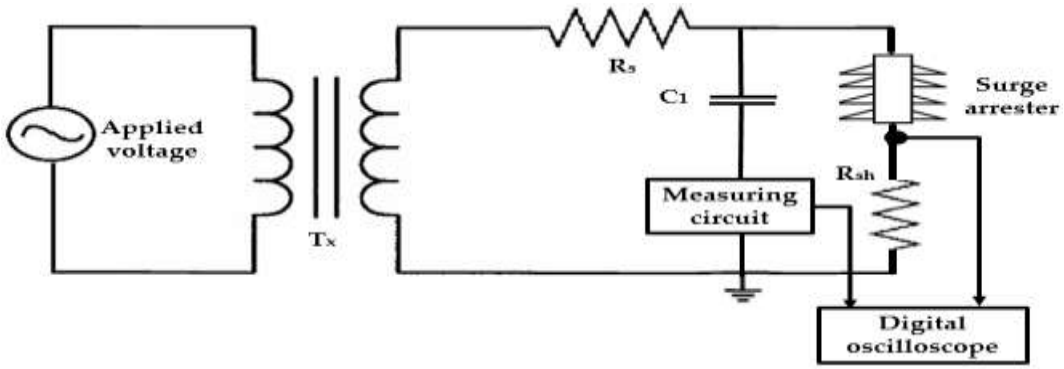

Figure 2: Experimental setup for leakage current measurement

Measurements of surge arrester leakage current were conducted under different applied voltages and conditions, as depicted in Table 2. For test sample 1, the applied voltage of 50 Hz AC sinusoidal was varied at 6, 7, 8, 9, and 10 kV while maintaining its temperature at 25 °C. The surge arrester was stressed for 30 min at 5 kVrms before any measurement was taken to ensure that quasi-static conditions were reached. One of the objectives of this work was to inspect the effect of pollution on the leakage current of the surge arrester. Hence, test samples 2 and 3 were prepared based on the pollution related to natural and anthropogenic sources. For test sample 2, the uncontaminated arrester was sprayed with water on the arrester surface. Different wetness's of the arrester were generated by adding water on the arrester surface in different quantity and the testing was under an applied voltage of 8 kVrms at 25 °C.

For test sample 3, the surge arrester was polluted by anthropogenic sources. The outer layer of the surge arrester was contaminated with dry sand, wet sand, salt sand and salt water and tested under an applied voltage of 50 Hz, 8 kVrms at 25 °C.

Table 2: Conditions of Each Test Sample

Test Sample	Conditions		
	Applied Voltage	Temperature	Surface Condition
1	50 Hz AC sinusoidal: 6, 7, 8, 9, and 10 kVrms	25 °C	Clean
2	50 Hz, 8 kVrms AC sinusoidal	25 °C	Dry, lightly wet, wet, very wet
3	50 Hz, 8 kVrms AC sinusoidal	25 °C	Dry sand, wet sand, salt sandand salt water

The wet sand was prepared by adding 200 g of sand into 150 ml of distilled water. The salt sand was a combination of 50 g of NaCl and 100 g of sand while for salt water, the solution consists of 50 g NaCl and 50 ml distilled water. For every pollution type, the arrester was cleaned and rinsed with water thoroughly before another type of pollution was applied. At the end of the experiment, the leakage current waveform recorded by the oscilloscope was used to extract the resistive and capacitive current using an improved time-delay addition method (ITDAM).

This method is more accurate and capable of extracting resistive and capacitive currents under applied harmonic voltages and based on the study, ITDAM can be utilized in offline or online measuring processes. This technique is based on the orthogonally between resistive and capacitive currents. The advantage of this method is that the harmonic components of the applied voltage are not ignored, where the resistive current is extracted from the total leakage current under applied harmonic voltages. The capacitive current is attained by shifting the total leakage current by 90°. Then, the resistive leakage current is obtained by subtracting the capacitive leakage current from the total leakage current. In this method, only the third and fifth harmonics of the applied voltage were measured. Also a three-dimensional (3D) 11 kV surge arrester model was developed in a finite element method (FEM) and was employed to simulate the leakage current in different conditions of the applied voltage, wetness and pollution. Measurements of surge arrester leakage current under different conditions were also conducted. They were used to compare with the simulation results to validate the FEA model.

3.2. Finite Element Analysis (Fea) Leakage Current Model

A three-dimensional, 11 kV ZnO surge arrester model was developed in finite element analysis as depicted in Figure 2. The COMSOL Multi-physics software was used for the FEA. The model was developed according to the exact dimensions of the surge arrester that was used in the measurement. The arrester comprises two ZnO blocks, a glass layer between the insulation and ZnO and aluminum caps at each end. The insulation material is made of silicone rubber and the whole model geometry was surrounded by a layer of air.

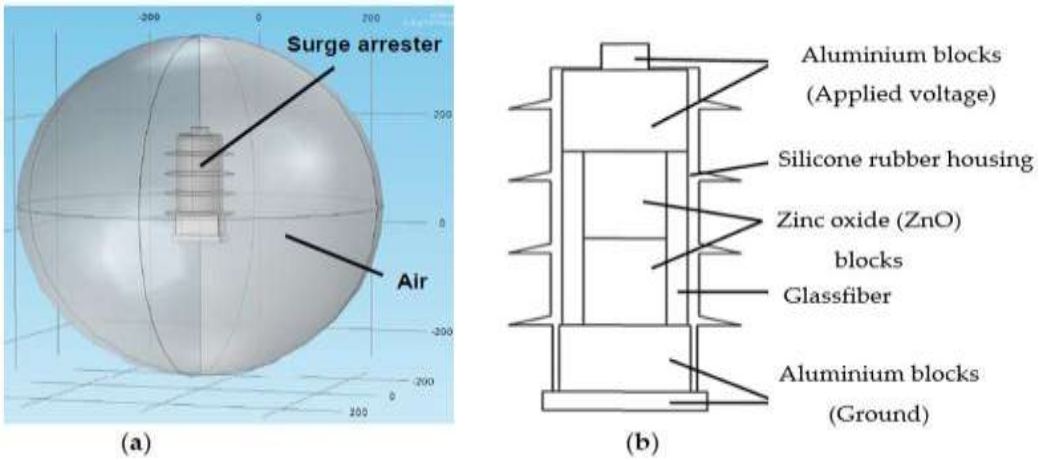

Figure 3: Surge Arrester Model; (a) Drawn in 3D; (b) Detailed Structure of the Model.

The electrical conductivity, σ and relative permittivity, εr of each material in the model were assigned as listed in Table 3. Since ZnO is a nonlinear element, the electrical conductivity of the ZnO blocks was assigned according to the measured V-I characteristics curve of the surge arrester during normal conditions, as shown in Figure 4, where their electrical conductivity is voltage-dependent. This curve is a fundamental approach in displaying the changes of resistance as a function of the voltage. Generally, the ZnO varistors spend their whole life in this region where conduction is very near to zero by means there is minimal leakage current flowing through the arrester.

Table 3: Properties of Each Material in the Model

Material	**Relative Permittivity, εr**	**Electrical Conductivity, σ (S/m)**
Air	**1**	**0**
Silicone rubber	11.7	1×10^{-12}
Aluminium	1	3.77×10^{7}
Glass	4.2	1×10^{-14}
Zinc Oxide	2250	From V-I curve

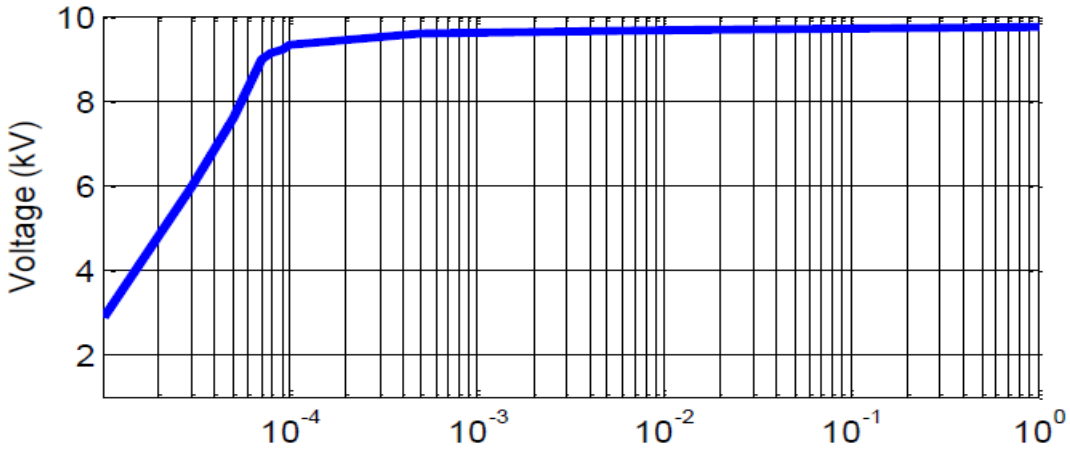

Figure 4: V-I Characteristics Curve of ZnO Varistor.

The boundary conditions of the model were set with relevant interface settings as shown in Table 4. A voltage with the presence of harmonic components was applied to the terminal of the arrester while the bottom of the arrester was grounded, whereby zero electric potential was applied. The outer side of the arrester was enclosed by air. All interior boundaries were set to continuity.

After the boundary and material of the model were assigned, the model was meshed. The FEA model estimates the solution of domain, boundary, edge and point of surge arrester model by using some elementary shape functions, which include tetrahedral, triangular, edge and vertex elements.

The shape function can be either constant, linear, or of higher order. In order to obtain accurate results, a finer or coarser mesh is required depending on the element order in the surge arrester model. Since the size of the triangular elements has substantial effect on the simulation time, the size of the triangular elements used was normal for air, finer for all domains of the model except for ZnO, which is extremely fine because it is the important element of the model. While constraining the potential on edges, it can produce a current outflow that is mesh-dependent. The meshing elements of the surge arrester are shown in Figure 5.

Table 4: Boundary Settings of the Model

Boundary	**Boundary Condition**
Terminal	Applied voltage
Ground	Zero electric potential
Interior boundary	Continuity
Air	Electric insulation

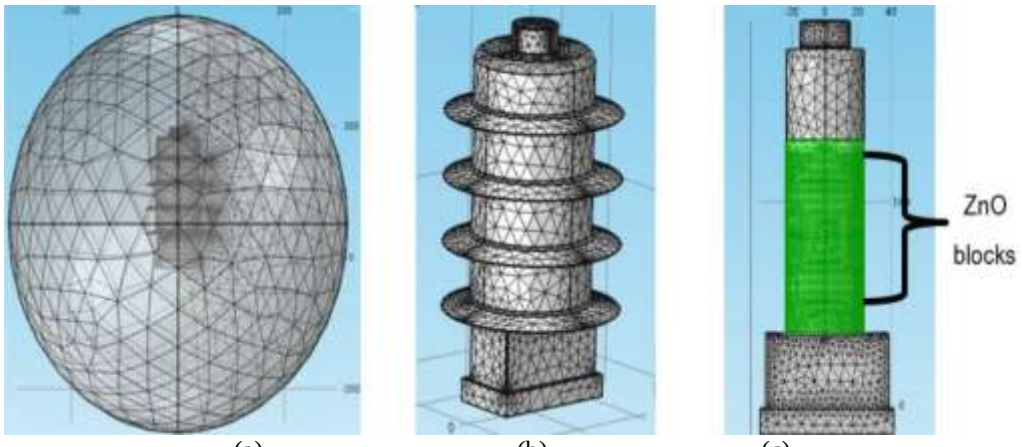

(a) (b) (c)

Figure 5: Meshing Elements in the Model; (a) Normal Elements for air; (b) Finer Elements for all domains of Surge Arrester; (c) Extremely fine Elements for ZnO.

The geometry of the surge arrester model was solved using partial differential equations (PDEs). The module employed in the model is the electric current module to obtain the electric field and current density distributions on the surge arrester. The leakage current was calculated through surface integration of the current

density, which was attained on the ground surface. Equations (1)–(6) were used by the FEA model to solve the problem as follows:

$$V = V_0 + \sum_{K=1}^{K} V_k Sin(k\omega t + \alpha_k) \quad (1)$$

$$\nabla \cdot J = Q_j \quad (2)$$

$$J = (\sigma + \varepsilon_0 \varepsilon_r \frac{\partial}{\partial_t}) E + J_e \quad (3)$$

Where J is the current density, $Q_j$is the current source, εr is the relative permittivity of the material, σ is the electrical conductivity, E is the electric field, Je is the externally generated current density, which equals to zero in the surge arrester model and V is the electric potential.

The problem to be solved in the model is governed by Maxwell's equation as follows:

$$\nabla \times E + \frac{\partial B}{\partial T} = 0 \quad (4)$$

By applying quasi-static assumptions, equation (3) becomes:

$$\nabla \times E = 0 \quad (5)$$

Since the electric field E is conservative and irrotational, E can be written as:

$$E = -\nabla V \quad (6)$$

IV. RESULTS AND DISCUSSION

This section presents the results that have been obtained from this work and the explanation of each result. These include the leakage current measurement results and comparison of leakage current amplitudes and signals between the measurement and simulation results.

4.1. Leakage Current Under Different Applied Voltages

The comparison between measurement and simulation results of the surge arrester total leakage current under different applied voltages are shown in Table 5 and Figure 6, while the resistive and capacitive leakage currents are shown in Tables 6 (a and b), and Figure 7 (a and b) respectively. Voltages from 6 kV to 10 kV were applied. It was found that the leakage current increases when the applied voltage is increased. This is fundamentally due to the direct proportionality between the voltage and current with an equivalent impedance, which is produced by the constant capacitive impedance, Z (I = V/Z). The percentage of error is calculated using the expression as

$$\text{Percentage error (\%)} = \left|\frac{I_{FEA} - I_m}{I_m}\right| \text{ x } 100 \quad (7)$$

Where I_{FEA} = the simulated value of the surge arrester leakage currents in μA and I_m = the measurement value of the surge arrester leakage current.

Table 5: RMS values of Total Leakage Currents for both Measurement and Simulated FEA Model

Applied Voltage (KV)	Measured Value (μA)	FEA Model (μA)	% Error
6	250	245	2.00
7	285	280	1.75
8	338	330	2.37
9	390	380	2.56
10	430	420	2.33

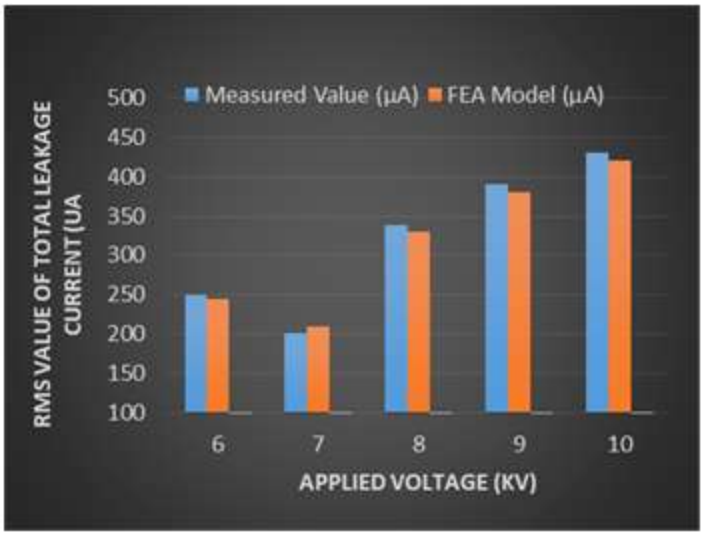

Figure 6: Comparison of RMS value of total leakage current between measurement and FEA model under different applied voltage amplitudes.

Tables 6: (a) Resistive leakage currents

Applied Voltage (KV)	Measured Value (µA)	FEA Model (µA)	% Error
6	17	16.5	2.94
7	23	22.5	2.17
8	26	25	3.85
9	33	32	3.03
10	44	43	2.27

(b) Capacitive leakage currents

Applied Voltage (KV)	Measured Value (µA)	FEA Model (µA)	% Error
6	233	230	1.29
7	285	281	1.40
8	312	309	0.96
9	347	344	0.86
10	386	382	1.04

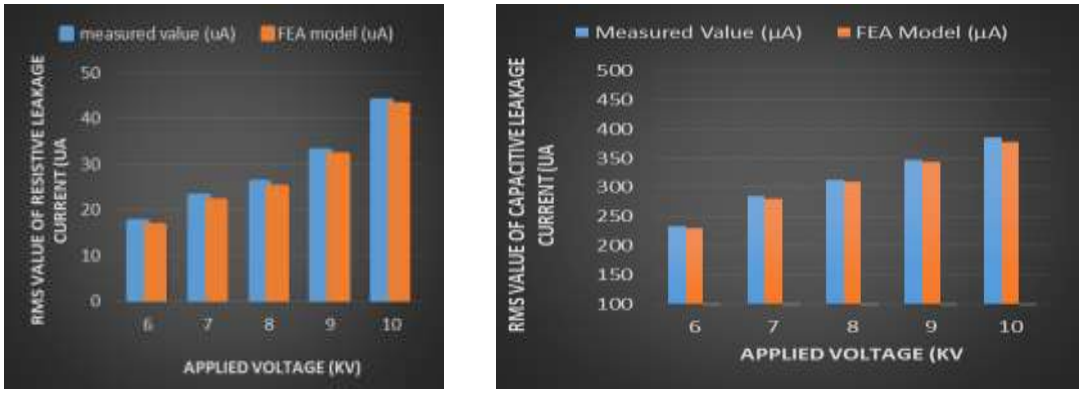

Figure 7: Comparison of RMS value of (a) Resistive; (b) Capacitive leakage current between measurement and FEA model under different applied voltage amplitudes.

The percentage error between the measurement and modeling was calculated based on equation (7) and are stated in Tables 5, 6 (a and b) respectively. According to the results, the average errors between the measurement and simulation for the total leakage current, resistive and capacitive leakage currents are 2.20%, 2.85% and 1.11% respectively. This indicates that there are significant closeness in values between the measurement and simulated results. Therefore, the proposed model of the surge arrester in this study under various applied voltages can be considered reasonable.

4.2. Leakage Current Under Different Wetness Conditions

The surge arrester was tested under different wetness conditions at 8 kVrms and at 25 °C. Table 7 and Figure 8 shows the results of total leakage currents value from the measured and simulated using the FEA model. From the results, it can be seen that the leakage current increases slightly when the arrester condition is much wet. This is due to the presence of more water droplets, which increase the conductivity along the surge arrester surface, providing an easier path for current to flow in the form of the negatively and positively charged

ions that are moving from one electrode to the other electrode. Tables 8 (a and b) and Figures 9 (a and b) shows the resistive and capacitive leakage currents components from the measured and simulated values. It can be seen that the resistive current component increases when there is more amount of water on the arrester surface. This humidification can also lead to moisture ingress into the surge arrester and degrade the lifetime of the surge arrester. However, there is not much variation in the capacitive current components under different wetness conditions. The errors between the measurement and simulation results using the FEA model are also shown in Tables 7 and 8 (a and b). The average percentage errors between the measurement and simulation results determined by equation (7) are 1.80% for the total leakage currents, 4.31% and 1.30% for resistive leakage currents and capacitive leakage currents, respectively.

Table 7: RMS values of Total Leakage Currents for both Measurement and Simulated FEA Model under wetness conditions

Total Leakage Current (µA) (µA)				
	Dry	Lightly Wet	Wet	Heavily Wet
Measured Value (µA)	338	342	350	364
FEA Model (µA)	331	336	342	360
% Error	2.07	1.75	2.29	1.10

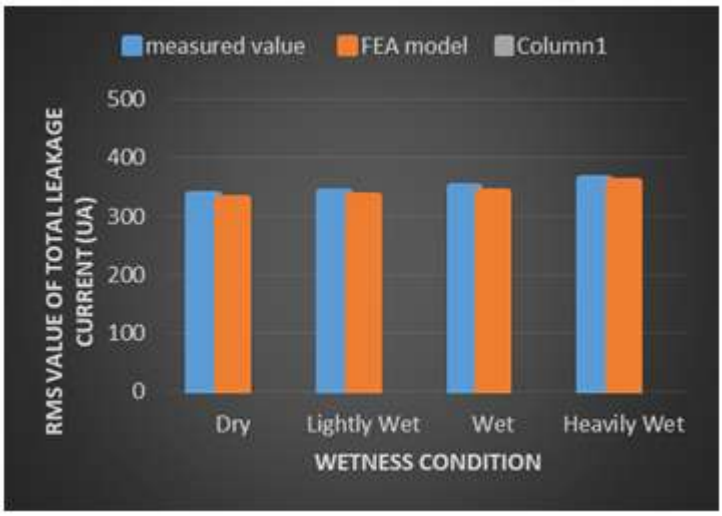

Figure 8: RMS value of the total leakage current between measurement and FEA model under different wetness conditions at 8 kVrms.

Tables 8: (a) Resistive leakage currents

Resistive Leakage Current (µA) (µA)				
	Dry	Lightly Wet	Wet	Heavily Wet
Measured Value (µA)	26	28	31	35
FEA Model (µA)	25	27.2	29.5	33
% Error	3.85	2.86	4.84	5.71

(b) Capacitive leakage currents

Capacitive Leakage Current (µA)				
	Dry	Lightly Wet	Wet	Heavily Wet
Measured Value (µA)	319	324	326	329
FEA Model (µA)	316	319	321	325
% Error	0.94	1.54	1.53	1.21

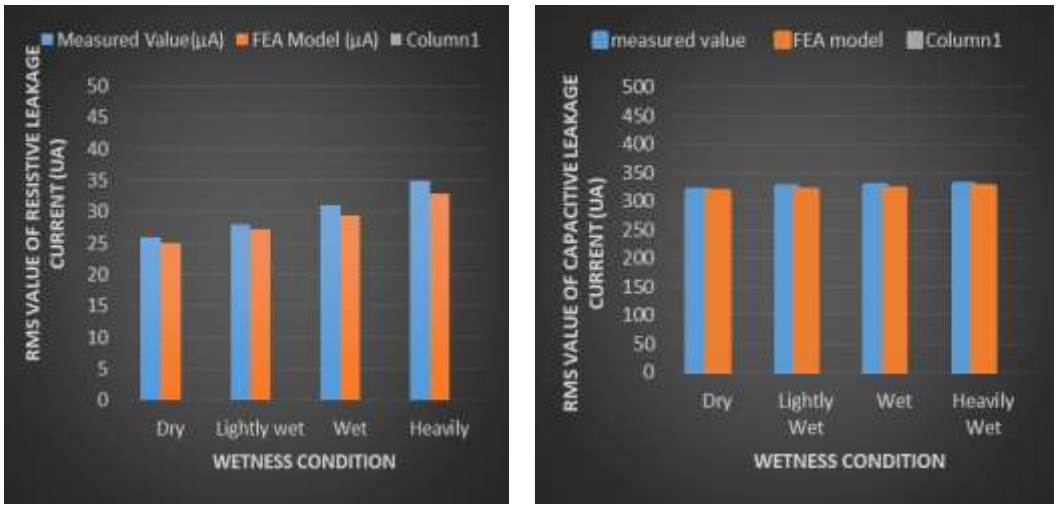

Figure 9: RMS value of the leakage current between measurement and FEA model under different wetness conditions at 8 kVrms for (**a**) resistive; (**b**) capacitive leakage current.

4.3. Leakage Current under Different Pollution Conditions

The leakage current behavior of the surge arrester under different pollution conditions is shown in Figure 10. From the measurement, the surface of the surge arrester was contaminated with dry sand, wet sand, salt sand and salt water. The salt sand is a blend of normal sand and salt, NaCl, with ratio of 2:1 while the salt water is an emulsion of NaCl and water with ratio of 1:1 with NaCl solution conductivity of 88 mS/cm. From the results, the presence of salt sand, salt water and wet sand on the surge arrester surface increases the total leakage current along the arrester surface. This is due to higher conductivity along the surge arrester surface provided by the salt and water, providing easier path for current to flow. The free ions created when salts are dissolved in the water will freely dissociate into ions. The Na+ and Cl− ions are moving through the water containing charges and therefore they conduct the electricity. Dry sand does not cause the leakage current to increase significantly because it has low conductivity. It can be concluded that increasing of leakage current is correlated to the increment of surface conductivity in pollution conditions. The error between the measurement and simulation results using the FEA model is also shown in Table 9. The average percentage of error is 1.40% for the total leakage current. This shows that there are significant closeness in values between the measurement and simulated results.

Table 9: RMS values of Total Leakage Currents for both Measurement and Simulated FEA Model under artificial polluted conditions.

Total Leakage Current (µA)					
	Clean	Dry Sand	Wet Sand	Salt Sand	Salt Water
Measured Value (µA)	338	340	336	335	360
FEA Model (µA)	335	338	330	330	352
% Error	0.89	0.59	1.79	1.49	2.22

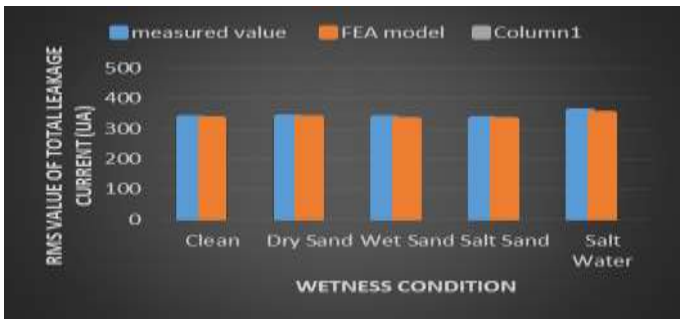

Figure 10: Comparison of RMS value of total leakage current between measurement and FEA model under different artificial pollution conditions.

V. CONCLUSIONS

In this study, the effect of different applied voltage, wetness conditions and pollution conditions on the surge arrester leakage current has been successfully evaluated using measurements and simulation models. It was found that the leakage current increases when the applied voltage is higher, wetness is higher and pollution conditions are worse.

A three-dimensional, 11 kV surge arrester model was successfully developed by finite element analysis (FEA) and was employed to obtain the total, resistive and capacitive leakage currents during normal operation under different conditions of applied voltage, wetness and pollution. The model was used to identify the surge arrester parameters which are influenced by these conditions. The leakage current amplitudes and signals obtained from the simulation of FEA model were also compared with the measurement results. It was found that the results obtained using the proposed. FEA model are significantly closed in values with the measurement results. Thus, the proposed FEA model for leakage current modeling in surge arrester in this study can be considered reasonable.

Hence, physical parameters of the surge arrester that influence the leakage current under different conditions of the surge arrester have been identified from the FEA model. The proposed model can also help in improvement of surge arrester design through the assessment of leakage current.

REFERENCES

[1]. Shariatinasab, R.; Ajri, F.; Daman-Khorshid, H. Probabilistic evaluation of failure risk of transmission line surge arresters caused by lightning flash. IET Gener. Transm. Distrib. **2014**, 8, 193–202.

[2]. Shariatinasab, R.; Safar, J.G.; Falaghi, H. Optimisation of arrester location in risk assessment in distribution network. IET Gener. Transm. Distrib. **2014**, 8, 151–159.

[3]. Vita, V.; Mitropoulou, A.; Ekonomou, L.; Panetsos, S.; Stathopulos, I. Comparison of metal-oxide surge arresters circuit models and implementation on high-voltage transmission lines of the Hellenic network. IET Gener. Transm. Distrib. **2010**, 4, 846–853.

[4]. Lee, B.H.; Kang, S.M.; Eom, J.H.; Kawamura, T. A Monitoring Device of Leakage Currents Flowing through ZnO Surge Arreters. Jpn. Soc. Appl. Phys. **2003**, 42, 1568.

[5]. Xu, Z.n.; Zhao, L.j.; Ding, A.; Lu, F.c. A Current Orthogonality Method to Extract Resistive Leakage Current of MOSA. IEEE Trans. Power Deliv. **2013**, 28, 93–101.

[6]. Lundquist, J.; Stenstrom, L.; Schei, A.; Hansen, B. New method for measurement of the resistive leakage currents of metal-oxide surge arresters in service IEEE Trans. Power Deliv. 1990, 5, 1811–1822.

[7]. Luo, Y.F. Study on Metal-Oxide-Arrester on-Line Monitoring Distributed-Control-System. Master's Thesis, School Electrical Engineering, Xi'an Jiao Tong University, Xi'an, China, 2003.

[8]. Heinrich, C.; Hinrichsen, V. Diagnostics and monitoring of metal-oxide surge arresters in high-voltage networks-comparison of existing and newly developed procedures. IEEE Trans. Power Deliv. **2001**, 16, 138–143.

[9]. Bajorek J, Knott M, Wyderka S (1992) Efficiency of Zno Arrester Models in Digital Simulation of Lightning overvoltages. ICLP Berlin, Germany, Pp: 265-270.

[10]. Khodsuz, M.; Mirzaie, M. An improved time-delay addition method for MOSA resistive leakage current extraction under applied harmonic voltage. Measurement 2016, 77, 327–334.

[11]. Khodsuz, M.; Mirzaie, M. Evaluation of ultraviolet ageing, pollution and varistor degradation effects on harmonic contents of surge arrester leakage current. IET Sci. Meas. Technol. 2015, 9, 979–986.

[12]. ABB, India. Selection guide for ABB HV surge Arresters zick oxide surge arresters, Technical information published SESWG/A 2300E, edition 2, 1991-2

[13]. Khodsuz, M.; Mirzaie, M. Harmonics ratios of resistive leakage current as metal oxide surge arresters diagnostic tools. Measurement 2015, 70, 148–155.

[14]. Seyyedbarzegar, S.M.; Mirzaie, M. Thermal balance diagram modelling of surge arrester for thermal stability analysis considering ZnO varistor degradation effect. IET Gener. Transm. Distrib. 2016, 10, 1570–1581.

[15]. Illias, A.Z.; Halim, S.A., Bakar, A.H.A.; Mokhlis, H. Determination of surge arrester discharge energy using finite element analysis method. IET Sci. Meas. Technol. 2014, 9, 693-701.

[16]. Bakar, A.; Halim, A.; Zainal Abidin, A.; Illias, H.A.; Mokhlis, H.; Abd Halim, S.; Nor Hassan, N.H.; Tan, C.K. Determination of the striking distance of a lightning rod using finite element analysis. Turk. J. Electr. Eng. Comput. Sci. 2016, 24, 4083–4097, doi:10.3906/elk-1311-175.

[17]. Schmidt W, Meppelink J, Richter B, Feser K, Kehl L (1989) Behavior of MO-Surge Arrester Blocks to Fast Transient. IEEE T Power Deliv 4: 292-300

[18]. Kershow S, Gaibrois GL, Stump KB (1989) Applying Metal-Oxide Surge Arresters on Distribution Systenm. IEEE T Power Deliv 4: 301-307

[19]. Shirakawa S, Endo F, Kitajima H, Kobayashi S, Kurita K (1988) Maintenance of surge Arrester by a Portable Arrester leakage Current Detector. IEEE T Power Deliv 3: 998-1003

J.O. Aibangbee" Modeling and Evaluation of Leakage Current Behavior of Metal oxide Surge Arresters under Various Applied Voltages and Polluted Conditions" The International Journal of Engineering and Science (IJES), 8.9 (2019): 11-20